Density functional study on the structural and thermodynamic properties of aqueous DNA-electrolyte solution in the framework of cell model

Ke Wang,[a] Yang-Xin Yu,[b] and Guang-Hua Gao
*Department of Chemical Engineering, Tsinghua University, Beijing 100084, People's Republic of China
and State Key Laboratory of Chemical Engineering, Tsinghua University, Beijing 100084,
People's Republic of China*

A density functional theory (DFT) in the framework of cell model is proposed to calculate the structural and thermodynamic properties of aqueous DNA-electrolyte solution with finite DNA concentrations. The hard-sphere contribution to the excess Helmholtz energy functional is derived from the modified fundamental measure theory, and the electrostatic interaction is evaluated through a quadratic functional Taylor expansion around a uniform fluid. The electroneutrality in the cell leads to a variational equation with a constraint. Since the reference fluid is selected to be a bulk phase, the Lagrange multiplier proves to be the potential drop across the cell boundary (Donnan potential). The ion profiles and electrostatic potential profiles in the cell are calculated from the present DFT-cell model. Our DFT-cell model gives better prediction of ion profiles than the Poisson–Boltzmann (PB)- or modified PB–cell models when compared to the molecular simulation data. The effects of polyelectrolyte concentration, ion size, and added-salt concentration on the electrostatic potential difference between the DNA surface and the cell boundary are investigated. The expression of osmotic coefficient is derived from the general formula of grand potential. The osmotic coefficients predicted by the DFT are lower than the PB results and are closer to the simulation results and experimental data. © *2008 American Institute of Physics*.
[DOI: 10.1063/1.2918342]

I. INTRODUCTION

A double-helix DNA carries two elementary negative charges per base pair in a living cell. Its stability and dynamics are significantly influenced by the composition of the ionic environment and the counterion distribution around it. To determine the physical properties of DNA in various electrolyte solutions, the classical dialysis equilibrium method[1] and some new experimental methods such as nuclear magnetic resonance,[2] x-ray diffraction,[3] and small-angle neutron scattering[4] have been used to examine counterion condensation around DNA. The shortcoming of these experiments is that we cannot obtain the detailed microscopic structure of mobile ions in the close vicinity of the surface of DNA.

To understand the microscopic structure of electric double layer (EDL) around the polyanionic DNA, various simulation methods have been developed in the past two decades.[5] Although the complicated models give some accurate descriptions of the structure of DNA,[6] the simple charged cylinder model combined with the primitive model of electrolyte solution can catch some basic characteristic properties of the EDL around DNA and is capable of reproducing with experiments at most conditions.[7,8]

The theoretical studies of physical properties of aqueous DNA solution started from the famous counterion condensa-

tion (CC) theory established by Manning.[9] This theory has been successfully applied in the calculation of the limiting behavior of thermodynamic properties[10,11] and now is extended to take account of both finite counterion concentration and actual structure of the array of discrete charges by Schurr and Fujimoto[12] with an alternative auxiliary assumption. In addition, Tan and Chen[13] presented a statistical mechanical model which accounts for the electrostatic and the exclude volume correlations of ions bound to a polyelectrolyte such as DNA.

The Poisson–Boltzmann (PB) equation is another mean-field theory for an aqueous electrolyte solution with the assumption that any ion corrections are unimportant.[14] The PB equation can be solved either analytically for simple geometries or numerically for more complicated physical models such as all-atom model of DNA,[15] etc. However, previous investigations have proven that the PB equation is invalid for the solution of high electrolyte concentration[16] or containing multivalent counterions since both charge and size correlations between small ions have evident effects on the total excess free energy under these conditions.[17]

Theories proposed to include the volume effect between small ions in aqueous DNA-electrolyte solutions can be classified into three groups. The first group is of the direct modifications of PB equation, in particular, the version of Bhuiyan and Outhwaite.[18] The second group is of integral equation theories,[19,20] usually with a closure of the hypernetted chain/mean spherical approximation (HNC/MSA).[20] For aqueous DNA solutions with high electrolyte concentrations or con-

taining multivalent counterions, the modified PB (MPB) and HNC/MSA theories generally give better predictions of structural and thermodynamic properties than the PB theory does.[19,21–23] The third group is of density functional theories (DFTs), which are easily implemented for various interactions between ions. It is generally based on minimization of the grand canonical potential of the system of interest. Several versions[24,25] of DFT have been proposed for inhomogeneous electrolyte solutions and in most cases, they are better than the PB theory. Recently, a DFT,[22,26] which is a combination of a modified fundamental measure theory (MFMT) proposed by Yu and Wu,[27] with the electrical interaction term obtained by using a quadratic Taylor expansion with respect to a uniform fluid,[25,26] has proved to be more accurate than the PB and HNC/MSA theories. This scheme has been used in our previous works[7,8,22,28] to study the structural and thermodynamic properties for the infinitely dilute DNA solutions.

In the present paper, we extend the DFT previously established[22] to the solution with finite DNA concentrations. Osmotic coefficient as an important thermodynamic property of polyelectrolyte solution has been investigated by experiments,[29,30] computer simulations,[31,32] and theoretical methods.[33,34] It is well-known that the cell model is the simplest way to obtain the thermodynamic properties of polyelectrolyte solution with finite polyelectrolyte concentrations. The cell model has been used not only to explain many experimental results but also to give theoretical support to modify the existing theories. The CC,[35] PB,[36] MPB,[21,31] and HNC/MSA[37] theories have already been implemented in the framework of cell model. The classical PB-cell model overestimates osmotic coefficients when compared to the computer simulation[32] and experiments.[30] However, no work on DFT in the framework of cell model has been reported except for a simplified version presented by us.[7] In the present work, the DFT proposed in our previous work[22] are combined with the cell model. The osmotic coefficient is computed from ion profile by using a general scheme derived from the grand potential. The predicted results are compared to the computer simulation and experimental results in literature.

The rest of this paper is organized as follows. In Sec. II, we give the basic assumptions of the cell model and then deduce the DFT in the framework of cell model. The physical model of DNA solution with simple ions is also given in this section. Numerical results for the ionic density profiles, electrostatic potential profiles, and osmotic coefficients at various solution conditions are presented in Sec. III. Some conclusions and perspectives for the future work are given in Sec. IV.

II. MODEL AND THEORY

A. Framework of cell model

In the study of aqueous DNA solution with finite concentrations, a number of DNA chains should be taken into account. To reduce the complicated many-particle problem of interacting polyions to an effective one-polyion problem, a cell model approximation is used to simply describe a
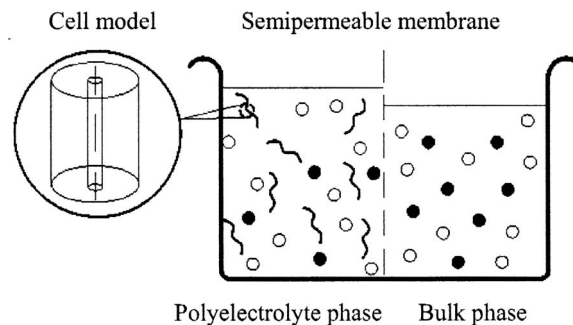

FIG. 1. Osmotic equilibrium between the polyelectrolyte phase and the bulk phase. The semipermeable membrane, which is permeable to simple ions and impermeable to polyelectrolyte, splits the solution into polyelectrolyte phase and bulk phase. The short curves, opened, and solid circles represent polyion, coion, and counterion, respectively.

polyelectrolyte solution as an ensemble of equal cylindrical cells.[38] The cell model approximation is closely related to the osmotic (Donnan) equilibrium if the cell boundary is regarded as a semipermeable membrane.[39] An illustration of osmotic equilibrium between the polyelectrolyte solution and the solution of small ions is shown in Fig. 1, where the solution containing polyelectrolyte and simple electrolyte (polyelectrolyte phase) is separated from an infinite reservoir of pure electrolyte solution (bulk phase) by a membrane which is permeable to all species but polyions. The equilibrium at constant temperature is achieved when the chemical potentials at both sides of membrane become equal. The polyelectrolyte phase is described within the framework of cell model. Deserno and von Grunberg[38] summarized the four basic assumptions of cell model: (i) the total charge within each cell is exactly 0, (ii) all cells have the same shape, (iii) the shape of cell should match the symmetry of the polyelectrolyte, and (iv) the interactions between different cells are neglected. These assumptions are accepted in the present work except the last one, for the short-range interaction between ions does not vanish at the cell boundary. In other words, the short-range interaction between the ions inside and outside the cell boundary should be taken into account. Based on assumption (ii) that all the cells are identical, a mirror boundary condition is used at the cell boundary instead, which allows the ion distributions out of the boundary to be mirrored from those inside. This modification has no effect on the long-range Coulombic interaction because the electroneutrality suggested by assumption (i) guarantees the vanishing point of electric field produced by polyion. Since the ion distributions outside the cell boundary are generated from those inside, the total partition function of the polyelectrolyte phase can also be factorized in the macroion coordinates. This modification also does not add any complexity of the cell model. It should be noted that sometimes, the system only includes the polyelectrolyte phase. In this case, a corresponding bulk phase can be imagined to dialyze with the polyelectrolyte phase.

B. Molecular model

The aqueous solution considered in this work contains DNA molecules with finite concentrations. We use the con-

centration of phosphate on the surface of DNA C_p as a measure of the concentration of DNA. The solution also contains one species of anion (coion) and one species of cation (counterion). The DNA molecule is modeled as an infinitely long, impenetrable and uniformly charged cylinder. Corresponding to B-form DNA, the radius of the hard cylindrical core of the DNA is $R_p = 0.8$ nm, and the charge spacing is $b = 0.17$ nm. Ions surrounding the DNA are modeled as charged hard spheres with various diameters σ_α. Therefore, the closest approach distance between the ion center and the DNA axis is $R_p + \sigma_\alpha/2$. The present work only involves simple spherical ions such as Na^+, K^+, Ca^{2+}, Mg^{2+}, and Cl^-, whose effective diameters are 0.376, 0.324, 0.52, 0.6, and 0.4 nm, respectively. They are taken from the work of Korolev *et al.*[40] for their good consistence with experimental data. The solvent water is modeled as a continuous structureless medium with invariant dielectric constant $\varepsilon = 78.4$ at any position, corresponding to that of the pure water at $T = 298$ K. All the radii and diameters involved in this paper are hydrated ones. The temperature of solution is $T = 298$ K. The radius of cell is calculated from C_p and b by $R_{cell} = \sqrt{\pi b C_p}$. To compare with the reported Monte Carlo simulation results of polystyrenesulfonate (PSS) solution, another set of parameters are used and explained in the text.

C. Density functional theory with cell model

In grand canonical ensemble, the system reaches equilibrium when the grand canonical potential Ω is at its minimum value. As commonly done, we enforce the cell electroneutrality by means of Lagrange multiplier method, and the actual canonical potential $\widetilde{\Omega}$ takes the form[33]

$$\widetilde{\Omega} = \Omega + \lambda \int_{\mathfrak{R}} \left[\sum_i z_i e \rho_i(\mathbf{r}) + q(\mathbf{r}) \right] d\mathbf{r}, \quad (1)$$

where the subscript $\mathfrak{R}$ denotes the whole region of the cell, z_i is valence of ion i, λ is the Lagrange multiplier, and $\rho_i(\mathbf{r})$ and $q(\mathbf{r})$ represent the density profile of ion i and charge distribution of DNA polyanion at position $\mathbf{r}$, respectively. The equilibrium density distributions of ion i, $\{\widetilde{\rho}_i\}$, are obtained from the Euler equation.

$$\left. \frac{\delta \Omega[\{\rho_i\}]}{\delta \rho_i(\mathbf{r})} \right|_{\widetilde{\rho}} + z_i e \lambda = 0. \quad (2)$$

The grand potential functional Ω involved in this work can be expressed as a functional of density profiles of ion species, through the Legendre transform

$$\Omega[\{\rho_i\}] = F[\{\rho_i\}] + \sum_{i=1}^{N} \int d\mathbf{r}[V_{Pi}(\mathbf{r}) - \mu_i]\rho_i(\mathbf{r}), \quad (3)$$

where $V_{Pi}(\mathbf{r})$ is the external field due to the DNA molecule, N is the total number of ionic species, μ_i is the chemical potential of ion i, and $F[\{\rho_i\}]$ represents the Helmholtz energy functional.

The Helmholtz energy functional should be expressed in a proper form. In general, it can be decomposed into four parts according to different types of interactions,

$$F[\{\rho_i\}] = F^{id}[\{\rho_i\}] + F_C^{ex}[\{\rho_i\}] + F_{hs}^{ex}[\{\rho_i\}] + F_{el}^{ex}[\{\rho_i\}], \quad (4)$$

where the first term on right of Eq. (4) is the ideal-gas contribution, obtained from classical statistical mechanics.[22,28] The second term is direct Coulomb contribution calculated by summing the electrostatic potential over the region of cell.[22,28] The third term denotes the hard-sphere contribution, which is calculated from the MFMT.[26] The last term of Eq. (4) is the electrostatic interaction obtained through a second-order functional Taylor expansion of the residual Helmholtz free energy around the corresponding bulk fluid,[26]

$$\beta F_{el}^{ex}[\{\rho_i\}] = \beta F_{el}^{ex}[\{\rho_i^b\}] - \int d\mathbf{r} \sum_{i=1}^{N} \Delta C_i^{(1)el}(\rho_i(\mathbf{r}) - \rho_i^b)$$

$$- \frac{1}{2} \int \int d\mathbf{r} d\mathbf{r}' \sum_{i=1}^{N} \sum_{j=1}^{N} \Delta C_{ij}^{(2)el}(|\mathbf{r} - \mathbf{r}'|)(\rho_i(\mathbf{r})$$

$$- \rho_i^b)(\rho_j(\mathbf{r}') - \rho_j^b), \quad (5)$$

where $\{\rho_i^b\}$ is the density of ion i in the bulk system, $\Delta C_i^{(1)el}$ and $C_{ij}^{(2)el}$ are direct correlation functions due to the residual electrostatic interaction, and $\beta = 1/k_B T$, where k_B is the Boltzmann constant. The $\Delta C_i^{(1)el}$ will disappear in the Euler equation and $\Delta C_{ij}^{(2)el}(r)$ can be explicitly evaluated by the MSA. The details of $\Delta C_{ij}^{(2)el}(r)$ have been described elsewhere.[41]

By making use of Eqs. (3)–(5), the Euler Eq. (2) becomes

$$\rho_i(\mathbf{r}) = \rho_i^b \exp \left\{ \frac{1}{k_B T}\left[-\frac{\delta F_{hs}^{ex}}{\delta \rho_i(\mathbf{r})} + \mu_{i,hs}^{ex,b} \right] - \frac{z_i e}{k_B T}[\psi(\mathbf{r}) + \lambda \right.$$

$$\left. - \psi^{CB}] + \sum_{j=1}^{N} \int d\mathbf{r}' \Delta C_{ij}^{(2)el}(|\mathbf{r}' - \mathbf{r}|)(\rho_j(\mathbf{r}') - \rho_j^b) \right\}, \quad (6)$$

where $\mu_{i,hs}^{ex,b}$ is the excess chemical potential of the bulk fluid due to the hard-sphere contribution, e is the electron charge, and $\psi(\mathbf{r})$ and ψ^{CB} are the local mean electrostatic potential and electrostatic potential at cell boundary, respectively. Generally, one can select a fluid of any position in the osmotic equilibrium system described by Fig. 1 as a reference fluid. Because the deduction of $\Delta C_{ij}^{(2)el}(r)$ by using MSA needs the fluid to be electroneutral and this condition is not always met within the cell, we select the corresponding bulk phase as a reference fluid.

According to the cell model assumption (iii), we take cell shape as cylindrical cell since DNA is considered as a charged cylinder. The electrostatic potential $\psi(r)$ is obtained from the solution of cylindrical Poisson equation within the cell. If the potential at the cell boundary is chosen as a reference, $\psi(r)$ can be expressed as

$$\psi(r) - \psi^{CB} = -\frac{4\pi e}{\varepsilon} \int_r^{R_{cell}} \ln\left(\frac{r'}{r}\right) \sum_i \rho_i(r') z_i r' dr', \quad (7)$$

where R_{cell} is the radial limit of the cell. The Lagrange multiplier λ becomes the so-called Donnan potential representing the potential drop across the semipermeable membrane.[33]
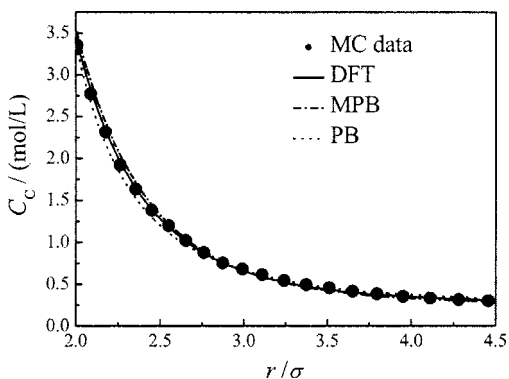
FIG. 2. Counterion concentration profiles around a polystyrenesulfonate in the salt-free solution with the polyelectrolyte concentration C_p =0.624 mol/l. The counterion is a monovalent ion. The solid circles, dashed, dash-dotted, and solid lines represent the results from Monte Carlo simulations (Ref. 21), PB-, MPB-, and present DFT-cell models, respectively.

If the short-range interactions are neglected, that is, the terms of $F_{hs}^{ex}[\{\rho_i\}]$ and $F_{el}^{ex}[\{\rho_i\}]$ vanish from Eq. (4), Eq. (6) reduces to the classical nonlinear PB equation in the frame of cell model,[33] i.e.,

$$\rho_i(r) = \rho_i^b \exp\left\{-\frac{z_i e}{k_B T}[\psi(r) + \lambda - \psi^{CB}]\right\}. \qquad (8)$$

It is not necessary to take the bulk phase as a reference fluid. Many studies take the fluid at cell boundary as a reference fluid. Then, the PB equation acquires the form[42]

$$\rho_i(r) = \rho_i^{CB} \exp\left\{-\frac{z_i e}{k_B T}\psi(r)\right\}, \qquad (9)$$

where ρ_i^{CB} denotes the density of ion i at the cell boundary.

To solve Eqs. (6) and (8), the concentration of small ions in bulk phase should be set at first. Moreover, λ (the Donnan potential) should be adjusted by trial and error to satisfy the cell electroneutrality. As mentioned above, in many studies including some experimental ones, only the polyelectrolyte phase is present. In other words, the ion concentrations of bulk phase are not known at first. However, the bulk concentration is related to the parameters of polyelectrolyte phase, such as polyelectrolyte concentration, average concentrations
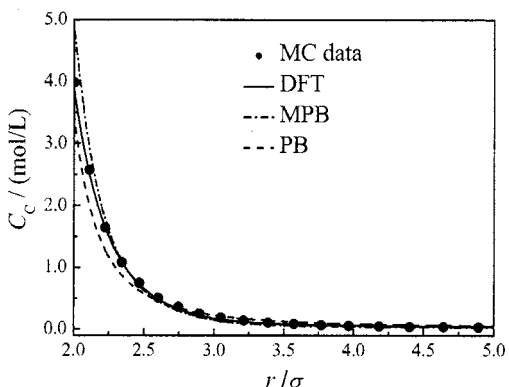

FIG. 3. Counterion concentration profiles around a polystyrenesulfonate in the salt-free solution with the polyelectrolyte concentration C_p =0.291 mol/l. The counterion is a divalent ion. The meaning of the symbols is the same as in Fig. 2.
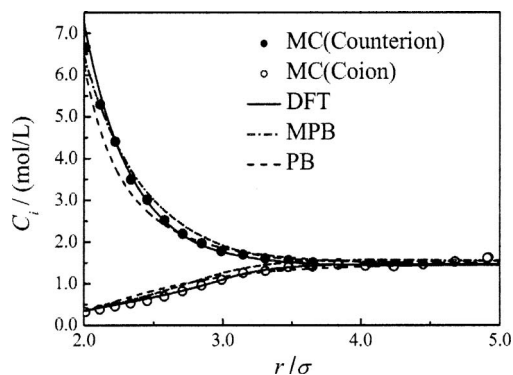

FIG. 4. Ion concentration profiles around a polystyrenesulfonate in the added 1:1 salt solution with the polyelectrolyte concentration C_p =0.624 mol/l and the salt concentration C_s=1.25 mol/l. The opened and solid circles represent the Monte Carlo simulation results (Ref. 21) for coion and counterion, respectively. The dashed, dash-dotted, and solid lines represent the theoretical results from the PB-, MPB-, and present DFT-cell models, respectively.

of ions, etc. In these cases, an iteration method is used to obtain bulk concentrations corresponding to the known polyelectrolyte phase.

D. Osmotic coefficient

Osmotic coefficient is usually used as a measure of non-ideality of the polyelectrolyte solution. We calculate the osmotic coefficients at various solution conditions from the ion profiles obtained in previous sections. The osmotic coefficient ϕ is usually obtained as a ratio of real solution pressure to the pressure of corresponding ideal gas,

$$\phi = p/p_{id}, \qquad (10)$$

where p is the pressure of polyelectrolyte solution and p_{id} is the pressure of corresponding ideal gas. p_{id} is calculated from the number densities of the mobile ions

$$p_{id} = k_B T \sum_i \rho_i. \qquad (11)$$

In the present work, the pressure is calculated from a general framework of grand canonical system,[33]

$$p = -\frac{\partial \widetilde{\Omega}}{\partial V} = -\omega^{CB}(\{\rho_i(\mathbf{r})\}, R_{cell}) - \lambda \sum_i z_i e \rho_i^{CB}, \qquad (12)$$

where V is volume and ω denotes local grand potential density,

$$\omega(\{\rho_i(\mathbf{r'})\}, \mathbf{r}) = f(\{\rho_i(\mathbf{r'})\}, \mathbf{r}) - \sum_i \mu_i \rho_i(\mathbf{r}), \qquad (13)$$

where f is the local free energy density, which can be obtained from the Helmholtz energy functional. It is expressed by

$$f = f^{id} + f_{hs}^{ex} + f_C^{ex} + f_{el}^{ex}, \qquad (14)$$

where f^{id}, f_{hs}^{ex}, f_C^{ex}, and f_{el}^{ex} denote the hard-sphere, Coulombic, and the electrostatic contribution to the local Helmholtz energy density, respectively. Based on our previous work, the four contributions are calculated from[22]

$$f^{\text{id}}[\{\rho_i\},\mathbf{r}] = k_B T \sum_{i=1}^{N} \rho_i(\mathbf{r})[\ln(\rho_i(\mathbf{r})\Lambda_i^3) - 1], \tag{15}$$

$$f_C^{\text{ex}}[\{\rho_i\},\mathbf{r}] = \frac{1}{2}\int d\mathbf{r}' \sum_{i,j} \frac{z_i z_j e^2 \rho_i(\mathbf{r})\rho_j(\mathbf{r}')}{\varepsilon|\mathbf{r}-\mathbf{r}'|}, \tag{16}$$

$$f_{\text{hs}}^{\text{ex}}[\{\rho_i\},\mathbf{r}] = k_B T \Phi^{\text{hs}}[n_\alpha(\mathbf{r})], \tag{17}$$

$$f_{\text{el}}^{\text{ex}}[\{\rho_i\},\mathbf{r}] = -\frac{k_B T}{2}\int d\mathbf{r}' \sum_{i=1}^{N}\sum_{j=1}^{N} \Delta C_{ij}^{(2)\text{el}}(|\mathbf{r}-\mathbf{r}'|)$$
$$\times \rho_i(\mathbf{r})\rho_j(\mathbf{r}'), \tag{18}$$

where $\Phi^{\text{hs}}[n_\alpha(\mathbf{r})]$ is the reduced excess Helmholtz energy density due to the hard-sphere repulsion and Λ_i is the thermal de Broglie wavelength of component i. In the framework of the PB equation, only the ideal-gas term and Coulombic term are involved. Therefore, the expression of pressure in the PB-cell model has a simple form[33]

$$p = k_B T \sum_{i}^{M} \rho_i(R_{\text{cell}}). \tag{19}$$

III. RESULTS AND DISCUSSION

In the present work, we consider the cases that the polyelectrolyte solutions contain only one counterion species or one counterion species plus a coion species. The former is called "salt-free" system and the latter is called "added-salt" system. The salt-free system of DNA and its counterions require a canonical formulation of the theory, i.e., DFT in a *NPT* or *NVT* ensemble.[43] However, the present DFT is constructed in a μVT ensemble. In fact, the salt-free system generally contains a very small amount of coions in the experiments. The equilibration of the polyelectrolyte solution against a salt reservoir will have different consequences depending on the DNA concentration. In this work, we use a salt reservoir with a very low coion concentration. We approximate the coion in the salt reservoir (corresponding bulk phase) as $10^{-3}C_p$, where C_p is the DNA concentration, i.e., the concentration of phosphate on the DNA surface in the electrolyte solution. In this case, the coion in the cell is much smaller than $10^{-3}C_p$, which has only a neglectable effect on the structural and thermodynamic properties of the solution.

A. Ion profile around polyion chain

To verify the DFT-cell model presented in this paper, the ion profiles calculated from the DFT are compared to molecular simulations and theoretical results. Figures 2–5 compare our DFT results with the MPB theory and Monte Carlo (MC) simulation data from Das *et al.*[21] for model PSS solutions. Another set of parameters is used for the PSS solutions, i.e., $T=298$ K, $R=0.6$ nm, and $b=0.252$ nm. All the ions are hard spheres with the same diameter $\sigma=0.4$ nm in Figs. 2–5. Figures 2 and 3 depict the ion profiles of monovalent and divalent counterions around polyion in salt-free solution, respectively. In both figures, the DFT accurately predicts the counterion profiles when compared to the MC
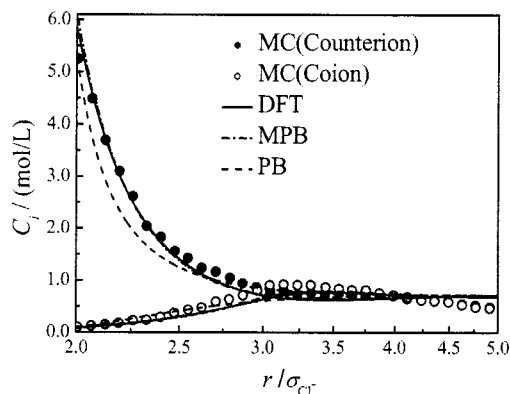

FIG. 5. Ion concentration profiles around a polystyrenesulfonate in the added 2:2 salt solution with the polyelectrolyte concentration C_p =0.624 mol/l and the salt concentration C_s=0.624 mol/l. The meaning of the symbols is the same as in Fig. 4.

results. We find that the MPB theory slightly overestimates the counterion concentration in the vicinity of the polyion, while the PB theory systematically underestimates it. Figures 4 and 5 depict the ion distributions around the polyelectrolyte in the solution with added single salt. These figures show that the DFT and MPB theory have compatible accuracy in the prediction of ion distributions in the polyelectrolyte solution with added salt. Moreover, the PB theory only gives a qualitative result and substantially underestimates the counterion concentration in the vicinity of the polyion. This is because both the DFT and MPB theory include the effect of ion correlations, while the PB theory does not.

The effect of polyion concentration is displayed in Fig. 6 for aqueous DNA solution without added salt. In the cases of both monovalent and divalent counterions, the polyelectrolyte concentration has little effect on the ion concentration in close vicinity of DNA chain but dramatically affects the ion concentration in the vicinity of cell boundary. The effect of ion size on ion distributions is demonstrated in Fig. 7. For monovalent counterions, the larger ions always have a higher local concentration than the smaller ones all over the space of the cell. However, in the case of divalent counterions, the order of the local concentration changes at a place approach-
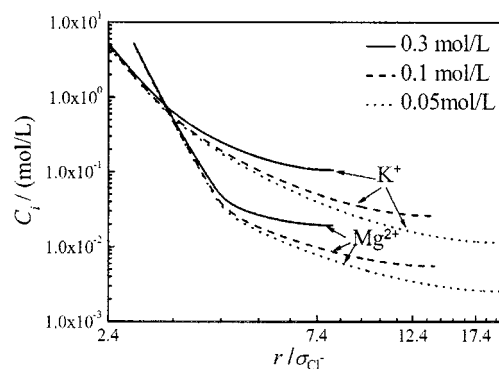

FIG. 6. The counterion distributions around DNA in the cell model of salt-free DNA solution as predicted from the DFT-cell model at different polyelectrolyte concentrations. The cases of K$^+$ and Mg^{2+} as counterions are displayed. Both x and y axes of this figure are plotted in logarithmic scale. The dotted, dashed, and solid lines represent the calculated results at DNA concentration C_p=0.05, 0.1, and 0.3 mol/l, respectively.
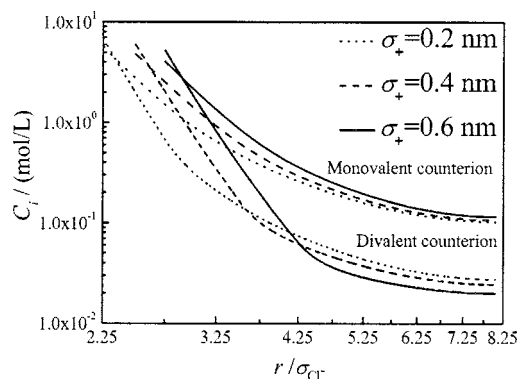
FIG. 7. The counterion concentration distributions around DNA in the cell model of salt free DNA solution as predicted from the DFT-cell model for different ion size. The dotted, dashed, and solid lines represent the results of counterions with ion diameters of 0.2, 0.4, and 0.6 nm, respectively. The polyelectrolyte concentration is fixed at 0.30 mol/l for all cases. Both x and y axes of this figure are plotted in logarithmic scale.

FIG. 8. Reduced electrostatic potential profiles around DNA in aqueous NaCl solutions within the cell. The concentration of DNA is C_p =0.5 mol/l, and the concentrations of Cl^- are C_{Cl^-}=0.01, 0.1, and 0.5 mol/l. The dashed and solid lines represent the results from the PB- and the present DFT-cell models, respectively.

ing the cell boundary, and the smaller counterions have a higher local concentration in the vicinity of cell boundary. As the valence of ion is increased, the nearest area around DNA becomes more crowded, and the volume effect of mobile ions makes greater contribution to the ion profiles. The volume effect trends to push ions toward a hard surface, which increases the ion density around DNA surface. This phenomenon is called wall effect. As the diameter of ion is increased, the volume that the ion takes becomes larger, and the wall effect becomes more obvious. The nearest ionic layers of the DNA are barely affected by the introduction of the finite cell and, therefore, do not differ from the previous work; i.e., the ion profiles at the DNA surface are not sensitive to the DNA concentration while the densities at cell boundary are.

B. Electrostatic potential

The ion distributions around DNA screen the electrostatic potential produced by DNA polyanion to some extent. In this work, we calculate the electrostatic potentials around DNA with the corresponding bulk phase as a reference; i.e., the electrostatic potential in the bulk phase is set to be 0. Figures 8 and 9 depict the electrostatic potential profiles within the cell in the case of added salt. As the concentration of added salt increases, the electrostatic potential profiles move toward zero. When the concentration of added salt increases to some extent, the electrostatic potential turns to be 0, which indicates that the ions in the cell has totally screened the electric field produced by DNA. In these cases, the region of bulk fluid exists within the cell and the concentration of DNA has no effect on the electrostatic potential profile. In the case of multivalent counterion, if the concentration of added salt is high enough, the phenomenon of *charge inversion* appears. That is a region where positive electrostatic potential exists within the cell, as shown in Fig. 9 for the case of added-salt concentration C_{Cl^-}=0.5 mol/l. The charge inversion can only be predicted by the theories which have included the ion correlations, such as HNC/MSA, MPB theory, and DFT.

Within the framework of cell model, the electrostatic potential difference between the DNA surface and the cell
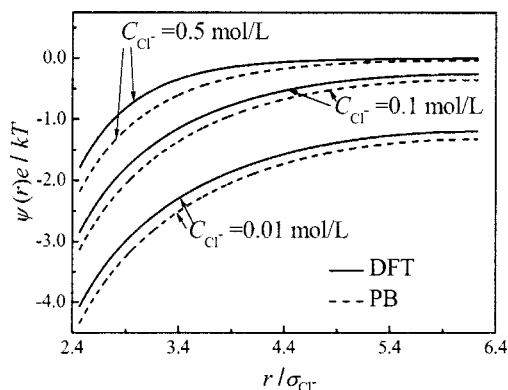
boundary, i.e., $\Delta\psi = \psi(R_p) - \psi(R_{cell})$, indicates the extent of the electric field screened by the ions within the cell. Figure 10 shows the effect of DNA concentration and ion size on $\Delta\psi$ in the salt-free solution. It is found that the divalent counterions have stronger ability to screen electrostatic potential produced by DNA polyion than monovalent ones do. A linear declination of DNA surface potential is found when the counterion diameter becomes larger. This indicates that the smaller counterions have stronger ability to screen the electrostatic potential produced than the larger ones do. This is because the same volume around DNA molecule trends to accommodate more small counterions. Thus, the smaller counterions neutralize the charge of DNA surface more rapidly along the radial direction. In all cases studied in this work, the nonlinear PB-cell model predicts a lower electrostatic potential around DNA than the present DFT-cell model does. It should be pointed out that the lower value means higher in absolute value, i.e., weaker screening within the PB theory. Furthermore, the nonlinear PB-cell model is unable to capture the interesting charge inversion phenomenon which is well represented by the present DFT-cell model (see Fig. 5).
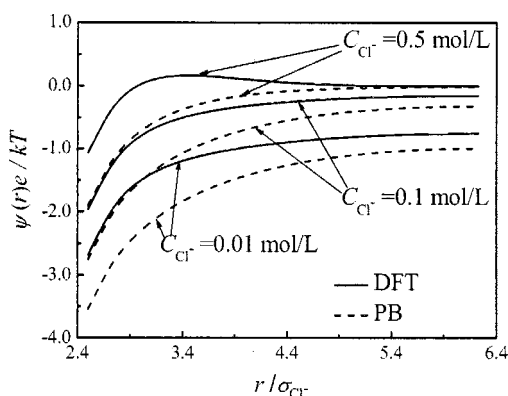

FIG. 9. Reduced electrostatic potential profiles around DNA in aqueous MgCl$_2$ solution within the cell. The concentration of DNA is C_p =0.5 mol/l, and the concentrations of Cl^- are C_{Cl^-}=0.01, 0.1, and 0.5 mol/l. The meaning of the lines is the same as in Fig. 8.
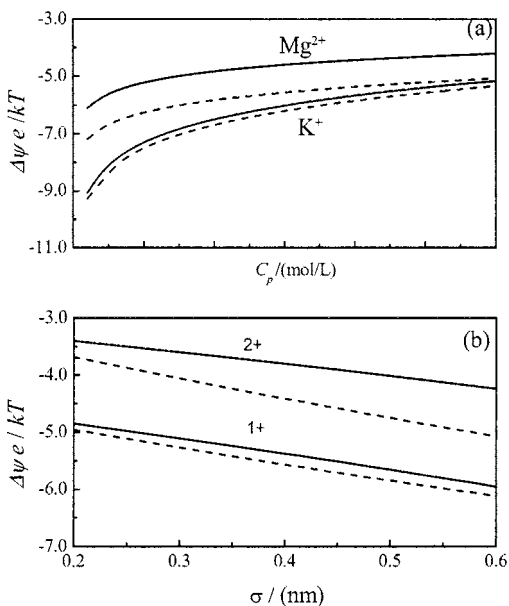
FIG. 10. Effect of DNA concentration and ion size on potential difference between the DNA surface and the cell boundary $\Delta\psi$ in the salt-free solution: (a) $\Delta\psi$ as a function of DNA concentration for counterion Mg^{2+} or K^+ and (b) $\Delta\psi$ as a function of counterion diameter in the salt-free solution with DNA concentration of $C_p=0.3$ mol/l. The dashed and solid lines represent the results from the PB- and DFT-cell models, respectively.

C. Osmotic coefficient

As concentration of DNA molecule becomes infinitely dilute (i.e., C_p is close to 0), the osmotic coefficient is close to the Manning limit. The Manning limit ϕ^0 is calculated from the following formula:[10]

$$\phi^0 = \begin{cases} 1 - \dfrac{1}{2}\xi, & \xi < 1 \\ 1/(2\xi), & \xi > 1, \end{cases} \qquad (20)$$

where ξ is the Manning parameter.

Antypov and Holm[32] simulated the osmotic coefficients of polyelectrolyte solutions, in which the polyelectrolyte is modeled as a stiff chain with one charge per monomer of unit length σ. The counterions were treated as point charges that could approach the monomers as close as 1σ. The Bjerrum length was set to 3σ. This value yields a Manning parameter $\xi=3$ and a limiting osmotic coefficient $\phi^0=0.167$ at infinite dilution. The comparison of our DFT-cell model results with their simulation data is presented in Fig. 11. It is found that the results from both the PB- and DFT-cell models reach this limit at infinite dilution. The results from the DFT-cell model are lower than those from the PB-cell model and are much closer to the simulation data. The deviations between the theoretical and simulated osmotic coefficients are partly due to that the different polyelectrolyte models are used in the two methods. In our cell model, the stiff polyelectrolyte is modeled as an infinite long charged cylinder, while in the simulation of Antypov and Holm,[32] the polyelectrolyte is regarded as a stiff chain composed of tangent hard spheres.

Figure 12 gives a comparison of the osmotic coefficients obtained from the PB- and DFT-cell models and the experiments[30] for DNA-electrolyte solutions. It is obvious
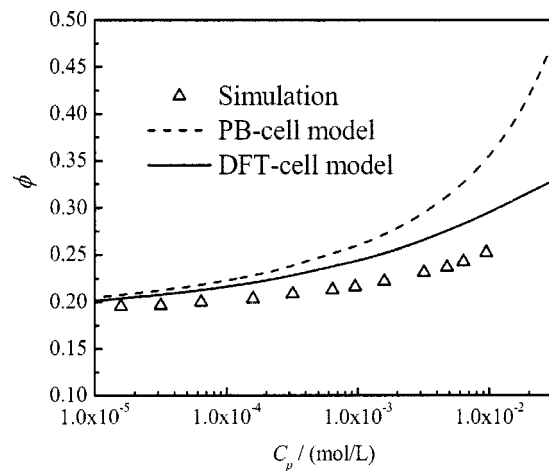

FIG. 11. Comparison of the theoretical predictions with the molecular simulations for the osmotic coefficient of model stiff polyelectrolyte solutions. The symbols, dashed, and solid lines represent the results from the molecular simulations (Ref. 32), PB- and DFT-cell models, respectively.

that the limiting osmotic coefficient is unity (i.e., $\phi^0=1$) in Fig. 12 rather than $1/(2\xi)$ in Fig. 11. This is because the polyelectrolyte phase is in equilibrium with bulk NaCl solution. This figure proves again that the osmotic coefficients from the DFT-cell model are lower than those from the PB-cell model. As mentioned in Sec. II D, the PB equation is a simplified case of DFT which neglects the ion correlations. Thus, from Figs. 11 and 12, we can conclude that the ion size correlations make the osmotic coefficient decrease to some extent, and the theory incorporating the ion size correlations gives more accurate prediction when compared to computer simulations or experimental results.

The ion size correlations become important at high ion concentration and for high-valence counterions in some polyelectrolyte solutions such as PSS or DNA. Their great effect on the potential difference between the DNA surface and the cell boundary has been demonstrated in Fig. 10. Here, we illustrate the effect of the ion size correlations on the osmotic coefficient of DNA-electrolyte solution in Fig. 13. The predictions of the DFT-cell model are always lower than those of PB-cell model, and the difference increases as the concentration of DNA is increased. The difference of
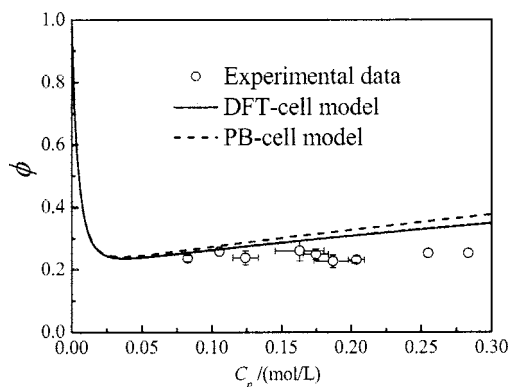

FIG. 12. Osmotic coefficient as a function of DNA concentration for an added-salt system. The polyelectrolyte phase is osmotically equilibrated with a 2.0 mmol/l NaCl bulk phase. The experimental results are from Raspaud et al. (Ref. 30).
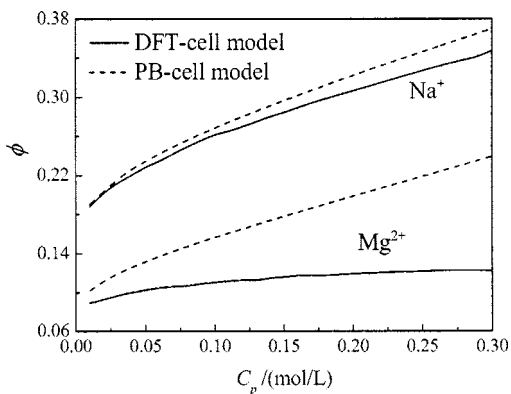
FIG. 13. Effect of DNA concentration on the osmotic coefficient in a DNA salt-free solution predicted from the PB- and DFT-cell models. The cases of Na^+ and Mg^{2+} as counterions are displayed.

results from two theories becomes more obvious in the case of divalent counterions. This indicates that ion size correlations make more contribution to the osmotic coefficient in divalent counterion system. It is evident that the volume packing effect makes more counterion accumulated in the vicinity of DNA surface, resulting in a lower counterion concentration at cell boundary and, thus, a lower osmotic coefficient. Because the DFT-cell model includes the ion size correlations between small ions, it is better than the standard PB-cell model in the case of high ion concentration and high-valence counterions in the polyelectrolyte solutions such as PSS and DNA.

IV. CONCLUDING REMARKS

In the present work, a DFT in the framework of cell model is proposed to investigate the structural and thermodynamic properties of aqueous DNA-electrolyte solution with finite DNA concentrations. The basic formulas of the DFT are inherited from our previous work.[22,28] In other words, the electroneutrality in the cell, which is a basic assumption of the cell model, leads to a variational equation with a constraint, and the Lagrange multiplier method is used to solve this problem. It proves that the corresponding bulk phase can be selected as a reference fluid required by the DFT, and in this case, the Lagrange multiplier coincides with the potential drop across the membrane (Donnan potential).

The numerical solutions of the DFT in the framework of cell model are compared to the computer simulation and modified PB theory. It is found that our DFT-cell model gives better prediction of ion profiles around rodlike polyion than the PB- or MPB-cell models do when compared to the MC simulation results. The ion profiles and electrostatical potential profile around DNA in aqueous electrolyte solutions are also investigated at different solution conditions. The effects of ion valence, ion size, and added-salt concentration on the electrostatic potential are in qualitative agreement with the case for infinitely dilute DNA solutions. The electrostatic potential difference between the DNA surface and the cell boundary increases with the increase in DNA concentration and linearly decreases with the increase in counterion diameter.

The osmotic coefficient is computed from ion profiles by using a general scheme derived from the grand potential. The results are compared to the previous computer simulation and experimental results. The results from the DFT-cell model are lower than those from the PB-cell model and are closer to the experimental results. It is concluded that the ion size correlations decrease the osmotic coefficient to some extent, and the theory incorporating the ion size correlations gives more accurate prediction when compared to computer simulation or experimental results. Since the effects of chain flexibility and conformation are not taken into account in this DFT-cell model, the coil structure and coil-globule transition with multivalent ions cannot be reproduced by this model. However, for the calculation of most properties such as ion-DNA binding, osmotic coefficient, etc., DNA in the solution can be regarded as stiff chains. From this point of view, the present DFT-cell model is a potential way to predict the thermodynamic properties of DNA-electrolyte solution at low to moderate DNA concentrations.

ACKNOWLEDGMENTS

[1] J. Shack, J. J. Robert, and J. M. Thompsett, J. Biol. Chem. **198**, 85 (1952).
[2] R. L. Kay, *Water: A Comprehensive Treatise*, edited by F. Franks (Plenum, New York, 1973).
[3] R. Das, T. T. Mills, L. W. Kwok, G. S. Maskel, I. S. Millett, S. Doniach, K. D. Finkelstein, D. Herschlag, and L. Pollack, Phys. Rev. Lett. **90**, 188103 (2003).
[4] S. S. Zakharova, S. U. Eqelhaaf, L. B. Bhuiyan, C. W. Outhwaite, D. Bratko, and J. R. C. van der Maarel, J. Chem. Phys. **111**, 10706 (1999).
[5] P. Mills, C. F. Anderson, and M. T. Record, Jr., J. Phys. Chem. **89**, 3984 (1985); J. C. G. Montoro and J. L. F. Abascal, J. Chem. Phys. **103**, 8273 (1995); V. Vlachy and D. J. Haymet, *ibid.* **84**, 5874 (1986); N. Korolev, A. P. Lyubartsev, A. Rupprecht, and L. Nordenskiold, J. Phys. Chem. B **103**, 9008 (1999); M. Deserno, F. Jimenez-Angeles, C. Holm, and M. Lozada-Cassou, *ibid.* **105**, 10983 (2001).
[6] S. Y. Ponomarev, K. M. Thayer, and D. L. Beveridge, Proc. Natl. Acad. Sci. U.S.A. **101**, 14771 (2004).
[7] Y.-X. Yu, K. Wang, and G.-H. Gao, Fluid Phase Equilib. **256**, 20 (2007).
[8] K. Wang, Y.-X. Yu, G.-H. Gao, and G.-S. Luo, J. Chem. Phys. **126**, 135102 (2007).
[9] C. F. Anderson and T. M. Record, Annu. Rev. Phys. Chem. **33**, 191 (1982).
[10] G. S. Manning, J. Chem. Phys. **51**, 924 (1969).
[11] G. S. Manning, Biophys. Chem. **7**, 95 (1977).
[12] J. M. Schurr and B. S. Fujimoto, Biophys. Chem. **101–102**, 425 (2002).
[13] Z.-J. Tan and S. J. Chen, J. Chem. Phys. **122**, 044903 (2005); S. J. Chen, Z.-J. Tan, S. Cao, and W.-B. Zhang, Wuli **35**, 218 (2006).
[14] D. L. Chapman, Philos. Mag. **25**, 475 (1913).
[15] B. Jayaram and D. L. Beveridge, Annu. Rev. Phys. Chem. **25**, 367 (1996).
[16] M. Fixman, J. Chem. Phys. **70**, 4995 (1979); S. L. Carnie and G. M. Torrie, Adv. Chem. Phys. **56**, 141 (1984); L. Degreve and M. Lozada-Cassou, Mol. Phys. **86**, 759 (1995).
[17] J. A. Schellman and H. R. Reese, Biopolymers **16**, 1415 (1977).
[18] L. B. Bhuiyan and C. W. Outhwaite, J. Chem. Phys. **116**, 2650 (2002).
[19] E. Gonzalez-Tovar, M. Lozada-Cassou, and D. Henderson, J. Chem. Phys. **83**, 361 (1985).
[20] E. Gonzalez-Tovar and M. Lozada-Cassou, J. Phys. Chem. **93**, 3761 (1989).
[21] T. Das, D. Bratko, L. B. Bhuiyan, and C. W. Outhwaite, J. Phys. Chem. **99**, 410 (1995).

[22] K. Wang, Y.-X. Yu, G.-H. Gao, and G.-S. Luo, J. Chem. Phys. **123**, 234904 (2005).

[23] J. Pinero, L. B. Bhuiyan, J. Rescic, and V. Vlachy, J. Chem. Phys. **127**, 104904 (2007).

[24] Y. Rosenfeld, J. Chem. Phys. **98**, 8126 (1993).

[25] C. N. Patra and A. Yethiraj, J. Phys. Chem. B **103**, 6080 (1999).

[26] Y.-X. Yu, J. Wu, and G.-H. Gao, J. Chem. Phys. **120**, 7223 (2004).

[27] Y.-X. Yu and J. Wu, J. Chem. Phys. **117**, 10156 (2002).

[28] K. Wang, Y.-X. Yu, and G.-H. Gao, Phys. Rev. E **70**, 011912 (2004).

[29] R. Podgornik, D. C. Rau, and V. A. Parsegian, Macromolecules **22**, 1780 (1989).

[30] E. Raspaud, M. da Conceicao, and F. Livolant, Phys. Rev. Lett. **84**, 2533 (2000).

[31] T. Das, D. Bratko, L. B. Bhuiyan, and C. W. Outhwhaite, J. Chem. Phys. **107**, 9197 (1997).

[32] D. Antypov and C. Holm, Phys. Rev. Lett. **96**, 088302 (2006).

[33] G. Téllez and E. Trizac, J. Chem. Phys. **118**, 3362 (2003).

[34] M. Muthukumar, J. Chem. Phys. **120**, 9343 (2004).

[35] J. M. Schurr and B. S. Fujimoto, J. Phys. Chem. B **107**, 4451 (2003).

[36] A. Katchalsky, Pure Appl. Chem. **26**, 327 (1971).

[37] V. Vlachy and D. A. McQuarrie, J. Chem. Phys. **83**, 1927 (1986).

[38] M. Deserno and H.-H. von Grunberg, Phys. Rev. E **66**, 011401 (2002).

[39] Z. Alexandrowicz and A. Katchalsky, J. Polym. Sci., Part A: Gen. Pap. **1**, 3231 (1963).

[40] N. Korolev, A. P. Lyubartsev, A. Rupprecht, and L. Nordenskiold, Biophys. J. **77**, 2736 (1999).

[41] K. Hiroke, Mol. Phys. **33**, 1195 (1977).

[42] G. V. Ramanathan and C. P. Woodbury, Jr., J. Chem. Phys. **82**, 1482 (1985).

[43] H. Wennerstrom, B. Jonsson, and P. Linse, J. Chem. Phys. **76**, 4665 (1982).